Environmental Research Laboratories

Air Resources
Atmospheric Turbulence and Diffusion Laboratory

Oak Ridge, Tennessee

MARCH 1974

METEOROLOGICAL EFFECTS OF THE COOLING TOWERS AT THE OAK RIDGE GASEOUS DIFFUSION PLANT

II. PREDICTIONS OF FOG OCCURRENCE AND DRIFT DEPOSITION

Steven R. Hanna

ATDL Contribution File No. 88.

U. S. DEPARTMENT OF COMMERCE
NATIONAL OCEANIC AND ATMOSPHERIC ADMINISTRATION

Meteorological Effects of the Cooling Towers at the Oak Ridge Gaseous Diffusion Plant

II. Predictions of Fog Occurrence and Drift Deposition

By

Steven R. Hanna
Air Resources
Atmospheric Turbulence & Diffusion Laboratory
P. O. Box E
Oak Ridge, Tennessee 37830

Abstract

The frequency of occurrence of fogs and the rate of deposition of chromate due to emissions from the cooling towers at the Oak Ridge Gaseous Diffusion Plant are calculated. Observations of drift deposition agree fairly well with calculated values. A detailed summary of significant findings is given at the end of the report.

1. Introduction

In part I of this report, source parameters of the cooling towers at the Oak Ridge Gaseous Diffusion Plant were described and plume photographs and hygrothermograph records were analyzed. Models of visible plume length were tested with observations. In part II, modelling of fog occurrence and drift deposition is described. The methods used are reviewed and outlined by Hanna (1974). To determine fog occurrence, the Gaussian plume dispersion model is used. To determine drift deposition, the trajectory of drops is calculated, accounting for drop evaporation. The drift deposition model is tested with observed data from April and June 1973 deposition experiments.

2. Fog due to Emissions from Cooling Towers at ORGDP

The water that is emitted from the cooling towers can condense to form fog or clouds. It can intensify an existing fog or clouds. Because latent heat is released in the condensation process, it is not strictly correct to treat the dispersion of water in the same manner as the dispersion of an inert substance such as suspended particles. However, since there is no accepted way to treat the dispersion of a substance which changes phase, the calculations in this report assume that water vapor is dispersed in the same way as an inert substance. The ground level fog concentrations calculated by this method are therefore likely to be too high, since the release of latent heat will cause the plume to rise.

In this section the climatological humidity variations are given and the frequency of occurrence of fog at distances out to 50 km from the towers is calculated.

2.1 Climatology of Moisture in the ORGDP Area.

Weather records at Knoxville have been taken since the late 1800's and are summarized in the Climatic Atlas of the U. S. (Environmental Data Service, 1968). The distribution of relative humidities by season and time of day is given in Figure 1. It is seen that the month with the most humid afternoons is January and the month with the most humid pre-dawn periods is July. However, since the saturation

vapor content or mixing ratio , m, is a strong function of temperature, as shown in Table 1, saturation due to the cooling tower moisture is most likely at cold temperatures.

Table 1

Variation of saturation mixing ratio m(gm water/kg air) with temperature.

T(°C)	-10	-5	0	5	10	15	20	25	30	35	40
m(gm/kg)	1.84	2.71	3.94	5.64	7.97	11.1	15.4	21.0	28.5	38.3	104.

As stated in the report ORO-99 (Holland, 1953) the average frequency of hours with rain in the Knoxville Area is 10%. From the Airway Meteorological Atlas (U. S. Weather Bureau, 1941), it is seen that the average frequency of hours with dense fog (visibility <1/4 mile) is .7% and with light fog (visibility < 6 miles) is 14%. However, the usual definition of fog (Neuberger, 1957) specifies a visibility less than 1 km. It is not possible to estimate this frequency from the available data.

The joint probability distribution of hourly wind speed, u(m/s), and saturation deficit, Δm (mass water vapor/mass air), given in Table 2, was calculated using 5 years of data from the X-10 meteorological station in Oak Ridge. Saturation deficit, Δm, is defined as the difference between the saturation mixing ratio and the actual mixing ratio.

Table 2

Joint Probability Distribution of Hourly Wind Speed and Saturation Deficit, X-10 Station.

Wind Speed Class m/s	Saturation deficit class (g/kg) / Effective saturation deficit (g/kg) / Effective wind speed u m/s	$\Delta m < .5 \frac{g}{kg}$	.5 - 1	1 - 2	2 - 4	4 +	Σ
	Effective saturation deficit (g/kg)	0	.75	1.5	3	6	
Calm	.5 m/s	.0721	.0347	.0459	.0440	.0435	.240
.5-2 m/s	1.5	.103	.0462	.0660	.0692	.121	.406
2-4.5 m/s	3.0	.0239	.0202	.0362	.0423	.112	.235
4.5-7 m/s	6.0	.00450	.00713	.0136	.0161	.0434	.0848
7-10 m/s	8.0	.00147	.00200	.00438	.00416	.0132	.0252
10+ m/s	10.0	.000343	.000648	.00149	.00170	.00503	.00920
Σ		.206	.111	.167	.177	.339	1

This distribution is probably very similar to that at the Oak Ridge Gaseous Diffusion Plant, since both sites are in valleys with ridges on either side. The wind rose measured at the Gaseous Diffusion Plant (from Hilsmeier, 1963) is given in Table 3.

Table 3

Wind Rose at Oak Ridge Gaseous Diffusion Plant. A North Wind Blows from the North.

Direction	N	NNE	NE	ENE	E	ESE	SE	SSE
Frequency	2%	9	24	6	4	2	3	2
Direction	S	SSW	SW	WSW	W	WNW	NW	NNW
Frequency	5%	6	12	5	6	5	6	3

The flow is strongly channeled in the NE-SW direction by the ridges in the area (see the map in Hanna and Perry, 1973). In general the Oak Ridge area is relatively humid with relatively light winds compared to the rest of the country, and the local flows are greatly influenced by local topography.

2.2 Source Terms and Diffusion Models.

Since beginning operation twenty years ago, the cooling towers at the Gaseous Diffusion Plant have continuously dissipated heat in the range from about 500 MW to 2000 MW. In this report, it is assumed that the heat dissipated is 1000 MW, corresponding to a total emission of water,

Q, of 4.6×10^5 g/sec (about 80% of the total heat dissipated is in the form of latent heat, as measured by Hanna and Perry, 1973).

The cooling towers can be described as a finite line source about 500 m long. A diagram of the cooling towers is given by Hanna and Perry (1973). Thus the line source strength is about 10^3 g/m sec. However at distances x downwind large compared to the length of the towers, they can be treated as a point source. In this report, we use point source formulas at distances from the source greater than 1 km, and line source formulas at distances from the source less than 1 km. The point source formula is easier to use.

When wind directions are reported in sixteen 22 1/2° sectors, the average yearly ground level concentration, χ(g/m^3), in each sector at a distance x(m) from a point source is given by the equation (see Gifford, 1968),

$$\chi = \sqrt{\frac{2}{\pi}} \frac{Qf}{\sigma_z U \frac{\pi x}{8}} e^{-h^2/2\sigma_z^2} \qquad (1)$$

where Q(g/sec) is source strength, f is the fraction of the time that the wind blows towards that sector, h(m) is effective plume height, and σ_z is the vertical dispersion length.

In part I of this report (Hanna and Perry, 1973) it was stated that the plume from these towers downwashes at wind speed, u, greater

than about 3 m/s. In these cases the effective plume height is close to zero. But visual observations suggest that the plume recovers from its initial downwash, and rises slightly beginning at downwind distances, x, of about 100 m. For cases when downwash does not occur, plume rise H can be calculated using Briggs (1969) equation:

$$H = 2.9\ (F/us)^{1/3} \qquad (2)$$

where $s(sec^{-2})$ is the stability parameter $(g/T_p)(dT_e/dz + .01^{o}C/m)$ and $F(m^4/s^3)$, proportional to the initial buoyancy flux is defined by:

$$F = w_o\ r_o^{\,2}\ \frac{g}{T_{po}}\ (T_{po}-T_{eo}) \qquad (3)$$

In these equations w_o, r_o, T_{po}, and T_{eo} are the initial plume vertical speed, plume radius, plume temperature, and environment temperature, respectively. T_p is the plume temperature and g is the acceleration of gravity. Hanna (1972) showed how equation (2) could be modified to account for the release of latent heat. Effective plume height h is the sum of plume rise H and tower height. Based on visual observations and calculations with Hanna's (1972) modification of equation (2), using known climatological values of U and s, the values of effective plume height in Table 4 were arbitrarily chosen.

Table 4

Effective Plume Heights as a Function of Wind Speed

Wind speed U(m/s)	.5 m/s	1.5	3	6, 8, 10
Effective plume height h(m)	200 m	100	25	12.5

A detailed measurement program should take place to better determine the plume rise at these towers. The straightforward application of equation(2)is complicated by the effects of multiple cells, latent heat, and downwash. Here it is assumed that the buoyancy from all the cells in a block can be added to give an effective buoyancy, but that the buoyancy from the three blocks does not combine. The blocks are separated by 200 m and 50 m.

At distances from the towers less than 1 km, a line source diffusion equation is used. Because of our lack of knowledge about the details of diffusion from such complicated sources, we decided to use the simplest basic formula. A complicated model is not justified until it is verified by an observation program. The sector average concentration due to the towers at short distances is thus given by the formula:

$$\chi = \sqrt{\frac{2}{\pi}} \frac{Qf}{\sigma_z U \left(\frac{\pi x}{8} + 500\text{m}\right)} e^{-h^2/2\sigma_z^2} \qquad (4)$$

where now f is defined as the fraction of the time the wind blows towards a sector of width ($\pi x/8$ + 500 m) at distance x from the towers.

The concentration, χ, on the plume axis very close to the tower openings is calculated by dividing the source strength, Q_p, by the plume velocity, $(w_o^2 + U^2)^{1/2}$, times the cross-sectional area, A, of the towers. The cross-sectional area equals tower width times tower length. The initial maximum concentration is therefore:

$$\chi = \frac{Q}{(w_o^2+U^2)^{1/2}A} = \frac{4.6\times10^5 \text{ g/sec}}{(w_o^2+U^2)^{1/2}(20\text{m} \times 500\text{m})} = \frac{46 \text{ g/m}^2\text{sec}}{(w_o^2+U^2)^{1/2}(\text{m/sec})} \qquad (5)$$

For an initial tower plume temperature of 100°F, the saturation water vapor content is about 50 g/m^3. This concentration should be regarded as an upper limit to the calculated concentrations. The maximum concentration will increase if the initial tower plume temperature increases.

In all these calculations, it is assumed that the atmospheric stability is nearly neutral. This assumption is most valid for long term averages or for cloudy, windy days. Briggs (1973) recommends that $\sigma_z(x)$ during these conditions is given by the relation:

$$\sigma_z = .07x/(1 + .0015x)^{.5} \qquad (6)$$

The smoothed distributions of dimensionless ground level concentrations calculated using equations (1), (4), and (6) are given in Figure (2)

for various classes of plume rise. As expected, an increase in plume rise greatly lowers the maximum ground concentration.

2.3 Average Annual Ground Level Excess Moisture due to Cooling Tower Operation

First, ground level excess moisture concentrations were calculated for each of the wind speed and plume rise classes in Tables 2 and 4. These values were then weighted by the wind direction and speed class frequency, to give the values in Figure 3, which are the average annual ground level excess moisture concentrations.

From Table 2, it is seen that the average annual saturation deficit (saturation mixing ratio minus actual mixing ratio) in this area is about 2 g/m^3. This figure is not exceeded on Figure 3. The ratio of average cooling tower excess moisture to average natural saturation deficit in the SW Direction is .4, .13, .06, .03, and .02 at distances from the towers of 1, 2, 5, 10, and 20 km, respectively. The city of Oak Ridge (population 30,000) which is the nearest center of population to the towers is about 10 km to the NE. Here the average contribution at the ground due to the cooling towers is about one percent of the average saturation deficit. However, it is obvious that at some times, when the saturation deficit is low, the excess moisture due to the cooling towers will exceed the saturation deficit and fog will occur.

2.4 Annual Frequency of Ground Level Fog due to Cooling Towers.

Depending on the definition of fog, the natural occurrence of fog and rain in this area is about ten to twenty percent. In this

saturated environment, the cooling tower plume may form a long cloud which releases much latent heat. Consequently, the diffusion of water in this thermodynamic system may not be similar to the diffusion of an inert substance. But, for simplicity of calculations, we will assume that the release of latent heat does not affect the diffusion. The resulting calculated fog frequencies are therefore probably conservative (too high).

Calculations of the ground level concentration of liquid water (excess water due to cooling towers minus saturation deficit) were made for the 30 joint classes of wind speed and saturation deficit listed in Table 2. These results will first be given in terms of hours of extra fog per year and then in terms of visibility.

It is assumed on the basis of known frequencies of rain and fog that the saturation deficit Δm is zero for the class $0 < \Delta m < .5$. These cases are examined separately. For the classes where $\Delta m > .5$ (i.e. no rain or fog) the hours of extra ground fog per year in the area around the towers are given in Figure 4. No extra fog occurs under these conditions farther than 2 km from the towers. At distances of 100 to 200 m from the towers, there is predicted to be about 100 extra hours of fog per year.

Figure 5 contains predictions of the hours per year when existing ground fog and rain is intensified by the cooling tower plumes. This effect extends to great distances from the towers. The maximum number on the figure is 408 hours per year with intensified fog, which occurs at distances 20 to 50 km SW of the towers. These calculations are highly tentative, since thermodynamic effects were not taken into account.

The average predicted fog concentrations and visibilities at certain distances from the towers are listed in Table 5. Visibility, V, is calculated from Trabert's (1905) formula:

$$V(m) = 2 \frac{g}{m^2 \mu m} \frac{D(\mu m)}{\omega(g/m^3)} \qquad (7)$$

where D is drop diameter in μm and ω is liquid water content in g/m^3. It is assumed that the drop diameter, D, equals 10 μm, typical of continental radiation fogs.

Table 5

Average Fog Concentrations Caused by Cooling Tower Operation and Corresponding Visibilities

x(m)	100	200	500	1000	2000	5000
$\omega(g/m^3)$	5.1	2.9	2.0	1.4	.61	.35
V(m)	4	7	10	15	33	57

Notice that the predicted visibilities are so low that a person could barely see a few meters. These visibilities are surely too low, since we have not accounted for removal. As liquid water concentration increases, droplets come together and are deposited as rain on the surface.

2.5 Occurrence of a Visible Plume Aloft

Another environmental effect of cooling towers is the possibility of an elevated visible plume decreasing the amount of sunlight reaching a station. The length of the visible plume was calculated

for each of the wind speed and saturation deficit classes in Table 2. For the case $\Delta m < .5$, which occurs 20% of the time, it is assumed that the plume extends indefinitely. This is an effect often observed during naturally foggy or rainy conditions. In Figure 6, the hours per year with a visible plume aloft are plotted. It is seen that in the SW direction at a distance of 1 km from the towers there are about 1500 hrs per year with a visible plume aloft. In Oak Ridge, 10 km to the NE, there are 240 hours per year with a visible plume aloft. Since there is also a natural cloud deck during most of these cases, the cooling tower plume is not very noticable.

The median visible plume length is calculated to be about 1 km. During the day, the observed visible plume length is only about .2 km (Hanna and Perry, 1973). But we are not able to observe the plume very well in the night, when the plume is the longest. Clearly an extensive observation program is needed to test the model predictions.

3. Drift Deposition

The mechanical draft cooling towers at ORGDP are about 20 years old and release a large amount of drift water, by today's standards. Hanna and Perry's (1973) and Environmental Science Corporation's (1973) measurement of the flux of liquid water from representative cells of these towers are summarized in Part I of this report series. A flux of

about 180 gm/sec of liquid water was observed at a typical cell on the K-31 towers. A total liquid water flux of about 3600 gm/sec was emitted during the period that our experiments were run. A more typical value for the liquid water flux would be about 14000 gm/sec, since usually the towers are dissipating more heat than was the case during the experimental period.

The concentration of sodium dichromate in the cooling water and the drift water is about 20 parts per million. A potential environmental problem is the deposition of chromate on the ground around the towers. In this section of the report, the techniques described by Hanna (1974) are used to estimate the deposition of drift water and chromates.

3.1 Mathematical Model of Drift Deposition.

The mathematical model of drift deposition that we developed accounts for the rise of the plume and entrainment of environmental air into the plume. The drop diameter changes due to differences between its vapor pressure and the vapor pressure of its environment. The model equations are solved numerically on the IBM 360/75 computer at Oak Ridge National Laboratory.

3.1.1 Plume Rise

The drop is assumed to originate from the center of the cooling tower cell opening. While it is in the plume, it experiences (see Briggs, 1969) a plume vertical speed, w, given by the relation:

$$w = \frac{.48\left[\dfrac{F_m}{\left(\frac{1}{3}+\frac{U}{w_o}\right)^2 U} + \dfrac{4Fx}{U^2}\right]}{\left[\dfrac{F_m x}{\left(\frac{1}{3}+\frac{U}{w_o}\right)^2 U^2} + \dfrac{2Fx^2}{U^3}\right]^{2/3}} \qquad (7)$$

where F_m is proportional to the momentum flux:

$$F_m = w_o^2 r_o^2 \tag{8}$$

The vertical motion of the plume ceases at a distance, x*, given by the equation:

$$x^* = 50m \left[F(m^4/s^3)\right]^{5/8}$$

For an individual cell at these particular cooling towers, $F = 25\ m^4/s^3$, and the distance x^* at which maximum plume rise is achieved is about 370 m.

Entrainment of environmental air causes the plume radius, R, to increase. The ratio of the volume flux of plume air, $V(z) = UR^2$, at any height to the initial volume flux, $V_o = w_o R_o^2$, is found by Hanna (1972) to equal:

$$\frac{V(z)}{V_o} = \left[1 + .5 \frac{(h-H)}{R_o} \frac{U^{1/2}}{w_o^{1/2}}\right] \qquad x \leq x^* \tag{9}$$

$$\frac{V(z,x)}{V_o} = \frac{U\left(R_o \left[\frac{w_o}{U}\right]^{1/2} + .5(h(x^*)-H) + C\,(x-x^*)\right)^2}{w_o R_o^2} \qquad x > x^* \tag{10}$$

where C is a constant proportional to the rate of spread of the plume after final rise is achieved at distance x^*.

Since the plume cools rapidly, we make the assumption that the saturation vapor pressure at the drop surface equals the saturation

vapor pressure of a drop at the temperature of the environment. To be strictly correct, the actual temperature of the plume should be used. Furthermore, we assume that the environment temperature and vapor pressure are constant, independent of height.

3.1.2 Drop evaporation

The drop will evaporate at a rate dependent on its diameter, the mass of solute in it, and the saturation and actual vapor pressures of the environment (see Fletcher, 1962, and Fleagle and Businger, 1964)

$$\frac{dD}{dx} = \frac{-8.0 \times 10^{-10}}{UD} \left[1 + .59 \sqrt{DV_g}\right] \left[p_s \frac{e^{\frac{2.0\times10^{-7}}{D}}}{\left(1+1.3\frac{M_s}{D^3}\right)} - p_a\right] , \qquad (11)$$

where D(cm) is drop diameter, U(cm/s) and V_g(cm/s) are wind speed and drop settling speed, M_s(g) is the mass of solute in the drop, and p_s (dynes/cm^2) and p_a(dynes/cm^2) are saturated and actual environmental vapor pressures. Vapor pressure is related to mixing ratio by:

$$p(\text{dynes/cm}^2) = 1.57 \times 10^6 \times m(\text{gm/gm}) \qquad (12)$$

As the drop evaporates, its fall speed changes. For small drop sizes, Stokes law is assumed to apply:

$$\begin{aligned} V_g &= 3.2 \times 10^5 D^2 && D < .0093 \text{ cm water drops} \\ V_g &= 8.0 \times 10^5 D^2 && \text{Sodium dichromate particles} \end{aligned} \qquad (13)$$

For larger drops, we use the following analytical approximations to the data given by Engelmann (1968, p 212):

$$V_g = 6816.D^{1.177} \qquad .0093 \text{ cm} < D < .068 \text{ cm}$$

$$V_g = 2155.D^{.746} \qquad .068 < D < .26 \text{ cm} \qquad (14)$$

$$V_g = 1077.D^{.224} \qquad .26 \text{ cm} < D$$

For small drops in a dry environment, the drop evaporates to a particle a few μm in diameter. If this happens, the motion of the particle is governed by diffusion and is treated similar to the diffusion of fog in section 2. The plume of particles dips down relative to the gaseous plume due to the slight settling of the particles. The deposition, $\omega(g/m^2 s)$, is then given by the relation $\omega = V_g \chi_o$. For V_g greater than 1 cm/s, the actual settling speed is used in equation (15). For V_g less than 1 cm/s, it is assumed that dry deposition occurred, and V_g is set equal to 1 cm/s in equation (15). More refined estimates of the dry deposition speed can be made following the recommendations of Van der Hoven (1968).

3.2 Computer Program

The above equations were programmed in Fortran IV for solution on the ORNL, IBM, 360/75 cumputer. It is assumed that all drops begin their motions at the center of an individual cooling tower cell. A downwind distance interval, Δx, of .5 m is used and calculations are carried out to a distance of 20 km from the towers. The total number of program statements is 95.

Input parameters are the saturated and actual mixing ratios of the environment, the wind speed, the tower height, and the initial momentum flux, buoyancy flux, radius, and vertical speed of the plume. In addition, several initial drop sizes are input.

The output consists of the final size of each drop or particle and the distance from the tower at which it strikes the ground. If the drop does not reach the ground, its final height and sizes are listed. Plume rise is also given.

3.3 Calculation of Chromate Deposition Rates.

The results of the computer program give information on the distance from the tower that a drop of a given size strikes the ground. From these numbers, it is possible to calculate the chromate deposition rate. For example, the program is run for a variety of initial drop diameters. It can be assumed that the drops of a given initial diameter fall uniformly between the point halfway between the points where that drop and the drop of next largestdiameter fall, and half way between the points where that drop and the drop of next smallest diameter fall. This concept is illustrated in Figure 7. If long term average deposition rates are desired, the sector averages can be employed, similar to the technique in equation (1). In this case the drops blowing in a given direction on a 16 point wind direction scale fall uniformly within a 22 1/2° angle centered on that direction. For simplicity, the 22 1/2 sector concept can also be applied to instantaneous deposition. This assumption is most correct for nearly neutral stability.

3.4 Results

Drift deposition rates are summarized for the period in June, 1973, during which observations were made, and for average annual conditions.

3.4.1 Drift Deposition During June, 1973, Experiments.

Measurements of drift deposition during the last week of June, 1973, are plotted on Figure 8. The ATDL (Hanna and Perry, 1973) and ESC (Shofner et al., 1973) observations, made with sensitive paper, were

generally from a location under the center of the visible plume. In contrast the BPNL (Lee et al., 1973) observations were made with a flat plate, and the station locations were fixed. Consequently, the BPNL stations were not often beneath the plume, which meandered about with the variable wind directions during this week.

The calculated drift deposition rates are also given in this figure. Deposition rates are interpolated between the curve for a single cell at x equal to 50 m and the curve for 20 cells at x equal to 500 m. Environmental conditions typical of those during the experiment are assumed:

$$m_s = .0238 \qquad m_a = .0138 \qquad U = 150 \text{ cm/sec}$$

Input source parameters have already been outlined by Hanna and Perry (1973).

The calculated and observed deposition rates agree fairly well at distances of 10 and 15 m, where it is likely that only one cell influences the deposition. The ESC (Shofner et al., 1973) measurements at distances of 35 and 80 m are about a factor of two greater than the calculated deposition rate, possibly because their sensitive paper was tilted a few degrees from the horizontal.

Since the ESC sensors were moved to insure that they were always beneath the plume, their measurements at these distances are greater than the BPNL (Lee et al, 1973) measurements. The BPNL sensors were beneath the plume only a fraction of the time, and their measured drift deposition rates are an order of magnitude less than the calculated

plume centerline deposition rates. If we assume that the plume blew over the BPNL sensors only 10% of the time, then calculated and observed deposition rates agree within a factor of two. The observations and the model estimates are therefore reconcileable at distances from 10 m to 1500 m from the tower.

3.4.2 Average Annual Drift Deposition

The average annual emission of drift water is about four times the emission assumed for the June, 1973, period. The drift deposition computer model was run for the following combinations of environmental parameters:

Summer day: $m_s = .0238$ $m_e = .0138$ U = 150 cm/s

Summer night: $m_s = .017$ $m_e = .017$ U = 50 cm/s

Winter day: $m_s = .0080$ $m_e = .0048$ U = 250 cm/s

Winter night: $m_s = .0037$ $m_e = .0031$ U = 100 cm/s

The four calculated values of deposition rate never differ by more than an order of magnitude. The average annual deposition rate at any distance x from the towers, plotted in Figure 8, is assumed to be given by the average of the deposition rate for the above four combinations. The resulting annual deposition rate of chromate in the area within 20 km of the towers is given in Figure 9. Figures are given for each 22 1/2° wind direction sector at distances greater than 1 km. Closer to the towers, the finite size of the line sources is accounted for by combining sectors. For example, at a distance of 50 m to the east of the tower center, the deposition rate is nearly the same whether the wind is from the west or northwest. The deposition rates close to the towers are listed in Table 6.

Table 6

Average Annual Chromate Deposition Rates ($\mu g/m^2 s$) Close to Cooling Towers

x (m)	East Sector	West Sector
5 m	23.2 $\mu g/m^2 s$	26.7
10 m	4.6	5.3
20 m	1.3	1.5
50 m	.23	.27
100 m	.08	.09

There is great variation in calculated deposition rate with distance from the tower. Chromate deposition varies from about 20 $\mu g/m^2 s$ near the tower to about 5×10^{-5} $\mu g/m^2 s$ at a distance of 20 km from the tower. At distances greater than 1 km (i.e., beyond the plant boundary) chromate deposition rate is calculated to be less than about 5×10^{-4} $\mu g/m^2 sec$, or 80 g/acre yr. The measured concentration of chromate in plants near the towers is being analyzed by F. Taylor of Oak Ridge National Laboratory and will be related to the deposition rates calculated above. These are the only data available to test the model for average annual deposition at this site.

3.5 Limitations

The deposition calculations must be regarded as tentative. In the first place there are no really good validation data for the model. Our method does not account for thermodynamic processes. To be strictly correct, the drops should originate at various locations across the mouth of the tower. In our technique, where all drops are started at the center of

the tower, a critical drop size is found during cases when relative humidity is less than 70%. Drops smaller than this critical size do not fall from the plume, but remain in the plume and eventually evaporate. Drops larger than this critical size fall from the plume and strike the ground within 200 m of the tower. A much more complicated model could be developed, but would not be justified by the current state of the art of the theory and measurement of drift deposition. The figures calculated here are probably accurate within a factor of five or ten.

4. Summary

The main results of this study can be summarized:

4.1 Average wind speed at this site is 2 m/s; average saturation deficit is 2 g/kg. This site has a relatively high potential for environmental problems with cooling tower plumes, due to the relatively low wind speed and saturation deficit.

4.2 The cooling towers are represented as a finite line source, with average total moisture (gaseous plus liquid) output of 4.6×10^5 g/sec. Average drift water output is 1.4×10^4 g/sec.

4.3 Neighboring plumes from the cells in a bank merge after a distance of about 50 m. Plumes from the three banks, initially separated by about 100 m, merge after a distance of about 500 m. Total plume rise averages about 200 m.

4.4 The ratio of average cooling tower excess moisture to average natural saturation deficit (2 g/kg) in the SW direction is .4, .13, .06, .03, and .02 at distances from the towers of 1, 2, 5, 10, and 20 km, respectively.

4.5 When latent heat is released during naturally rainy or foggy conditions, a cloud forms aloft with constant base height. This occurs about ten to twenty per cent of the time.

4.6 When naturally occuring rain or fog is absent, it is predicted that the cooling towers will cause about 100 extra hours of fog per year at distances of 100 to 200 m from the towers. The standard Gaussian plume model is used to make these predictions. No extra fog is predicted to occur under these conditions at distancesgreater than 2 km from the towers.

4.7 A visible plume aloft is calculated to occur over the city of Oak Ridge, 10 km to the NE, about 240 hours per year. During almost all of this time, a natural cloud deck will also be present.

4.8 Drift deposition is calculated using the Gaussian plume model for drops with diameters less than 200 μg. The trajectory approach is used for larger drops. The variation of vertical speed in the plume and the evaporation of drops are accounted for.

4.9 Predictions of chromate deposition at distances from 10 m to 1500 m from the towers agree fairly well with observations during the June, 1973, experiment.

4.10 Calculated average annual chromate deposition rates vary from about 20 $\mu g/m^2 s$ at distance of 5 m from the towers to 10^{-4} $\mu g/m^2 s$ at a distance of 20 km from the towers.

5. Acknowledgements.

This research was performed under an agreement between the National Oceanic and Atmospheric Administration and the Atomic Energy Commission.

W. M. Culkowski of this laboratory calculated the joint distribution functions of wind speed and saturation deficit. S. G. Perry, an Oak Ridge Associated Universities summer trainee at this laboratory, took part in the initial development of the drift deposition model. The cooperation of G. Kidd and T. Shapiro of the Oak Ridge Gaseous Diffusion Plant is gratefully acknowledged.

References

Briggs, G. A., 1969: Plume Rise, AEC Critical Rev. Series, USAEC-TID-24635, available from Clearinghouse, Springfield, Va., 22151, $3.00, vi + 81 pp.

Briggs, G. A., 1973: Diffusion Estimation for Small Emissions, draft of a manuscript to be published in the AEC critical review series, available as ATDL Contribution No. 79, P. O. Box E, Oak Ridge, Tn., 37830, 59 pp.

Engelmann, R. J., 1968: The calculation of precipitation scavenging, Meteorology and Atomic Energy 1968, edited by D. Slade, USAEC TID-24190, available for $6.00 from Clearinghouse, Springfield, Va., 22151, pp 208-221.

Environmental Data Service, 1968: Climatic Atlas of the United States, U. S. Dept. of Commerce, price $4.25 from Superintendent of Documents, U. S. Government Printing Office, Washington, D. C. 20402, 80 pp.

Fleagle, R. G. and J. A. Businger, 1963: An Introduction to Atmospheric Physics, Academic Press, Inc., New York, pp 79-108.

Fletcher, N. H., 1962: The Physics of Rainclouds, Cambridge Univ. Press, 386 pp.

Gifford, F. A., 1968: An outline of theories of diffusion in the lower layers of the atmosphere, chapter 3 in Meteorology and Atomic Energy 1968, D. Slade, ed., available as TID-24190 for $6.00 a copy from Clearinghouse, Springfield, Va., 22151, pp 66-105.

Hanna, S. R., 1972: Rise and condensation of large cooling tower plumes. J. Appl. Meteorol., 11, 793-799.

Hanna, S. R., 1974: Fog and drift deposition from cooling towers, to be published in Nuclear Safety, March-April 1974 issue.

Hanna, S. R. and S. G. Perry, 1973: Meteorological Effects of the Cooling Towers at the Oak Ridge Gaseous Diffusion Plant. I. Description of Source Parameters and Analysis of Plume Photographs and Hygrothermograph Records, available as ATDL Contribution No. 86, P. O. Box E, Oak Ridge, Tn. 37830, 30 pp + 10 figs.

Hilsmeier, W. F., 1963: Supplemental Meteorological Data for Oak Ridge. ORO-199, Division of Technical Information, USAEC, available from ATDL, P. O. Box E, Oak Ridge, Tn. 37830, 57 pp.

Holland, J., 1953: A Meteorological Survey of the Oak Ridge Area, ORO-99, Division of Technical Information, USAEC, 584 pp.

Lee, R. N., J. W. Sloot, and M. A. Wolf, 1973: Measurements of Chromate Resulting from Cooling Tower Drift at the Oak Ridge Gaseous Diffusion Plant, Final Report prepared for Union Carbide Nuclear Co. (AEC Contr. No. AT (45-1)1830) by Battelle Pacific Northwest Lab., Richland, Wa., 99352, 14 pp.

Neuberger, H., 1957: Introduction to Physical Meteorology. The Pennsylvania State University, University Park, Pa., 271 pp.

Shofner, F. M., G. O. Schrecker, and K. R. Wilber, 1973: Characterization of Drift Emissions and Drift Transport for Representative Cells of K-31 and K-33 Cooling Towers. Final Report prepared for Union Carbide Nuclear Co. by Environmental Systems Corp., P. O. Box 2525, Knoxville, Tn., 37901, 66 pp.

U. S. Weather Bureau, 1941: Airway Meteorological Atlas for the United States, U. S. Department of Commerce, W. B. Report No. 1314.

Van der Hoven, I., 1968: Deposition of particles and gases, Meteorology and Atomic Energy 1968, edited by D. Slade, USAEC TID-24190, available for $6.00 from Clearinghouse, Springfield, Va., 22151, pp 202-208.

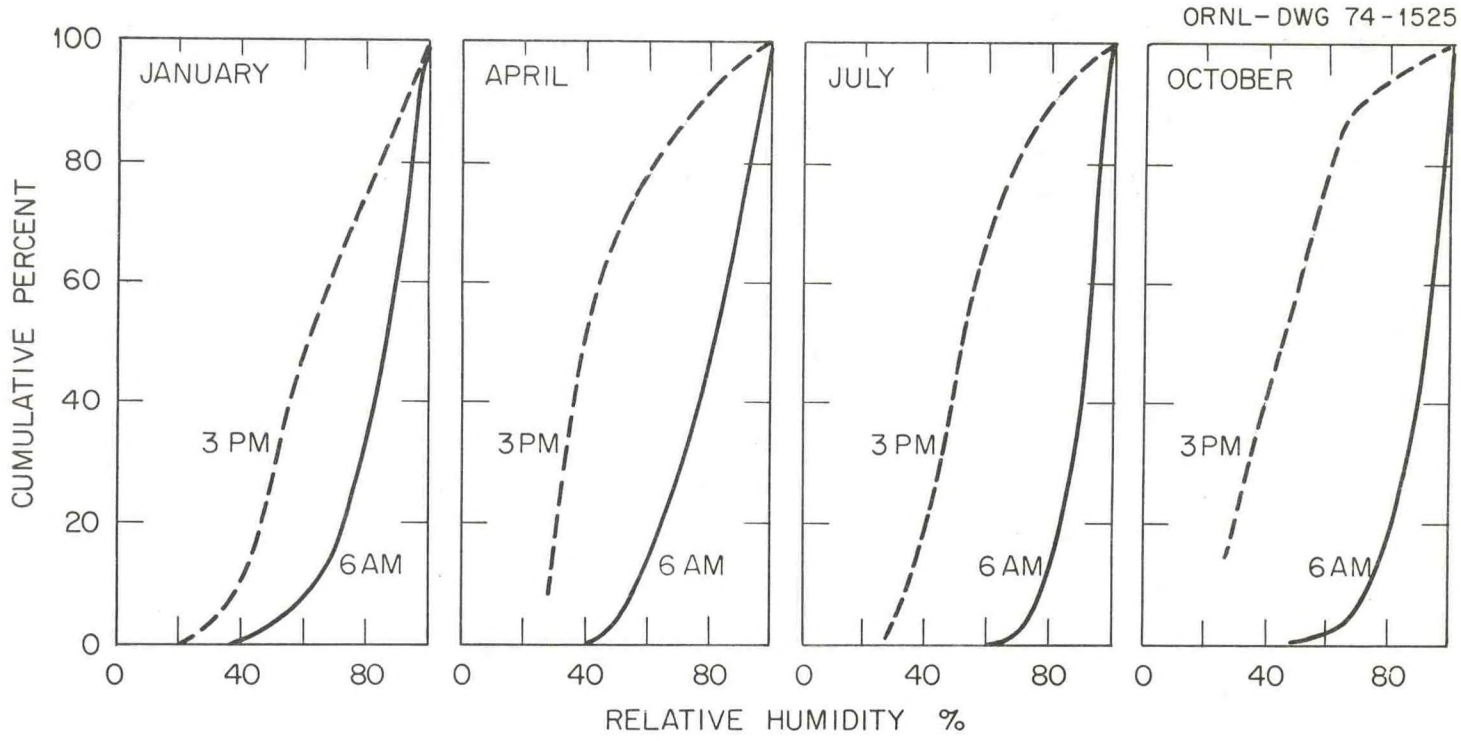

Figures 1: Distribution of relative humidity by season and time of day, in Knoxville, Tn. (From Environmental Data Service, 1966).

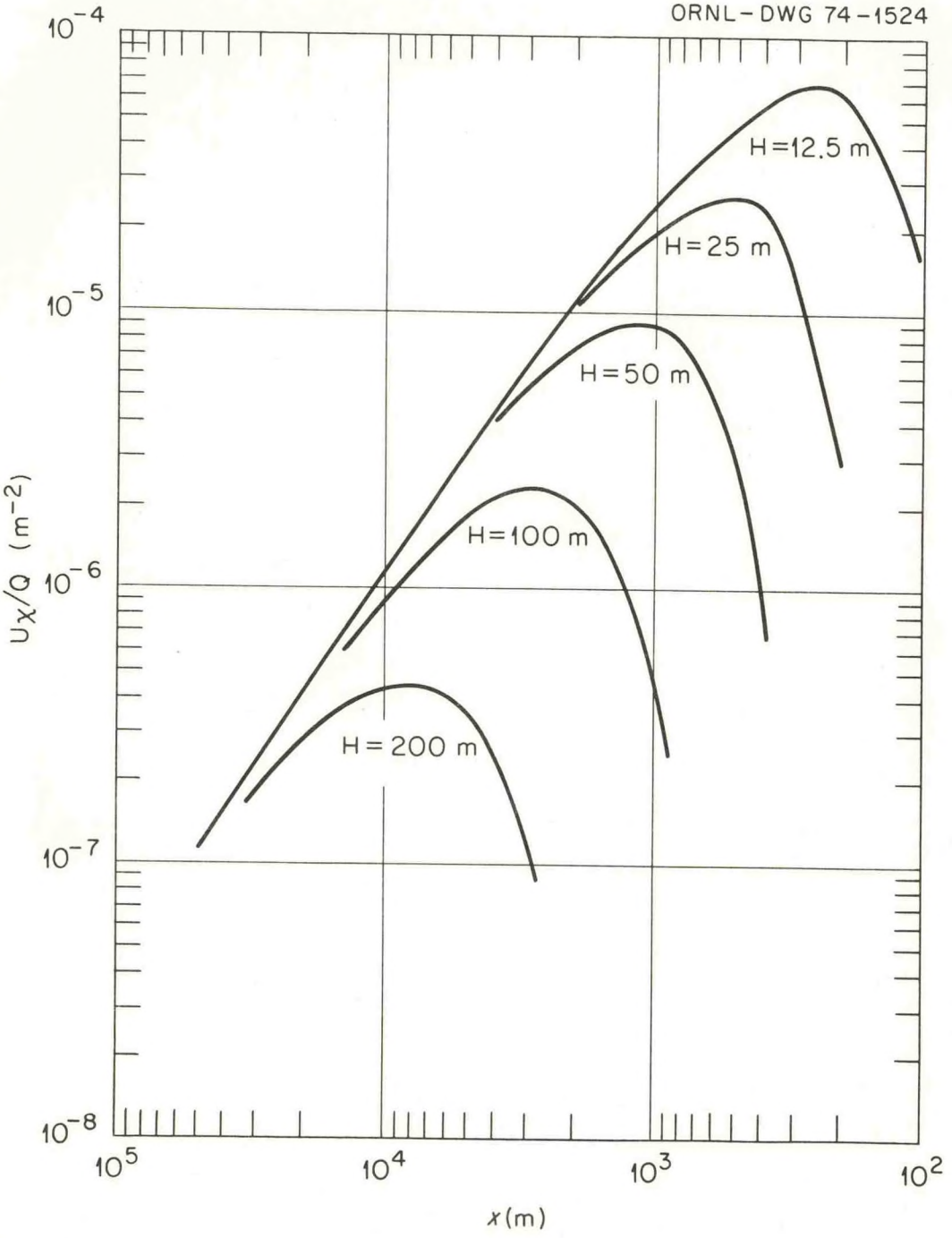

Figure 2: Curves of $\chi U/Q(m^{-2})$ as a function of downwind distance x, for neutral stability. Sector width is 500m + $\pi x/8$. Vertical dispersion parameter σ_z equals .07 x /(1+.0015x)$^{.5}$.

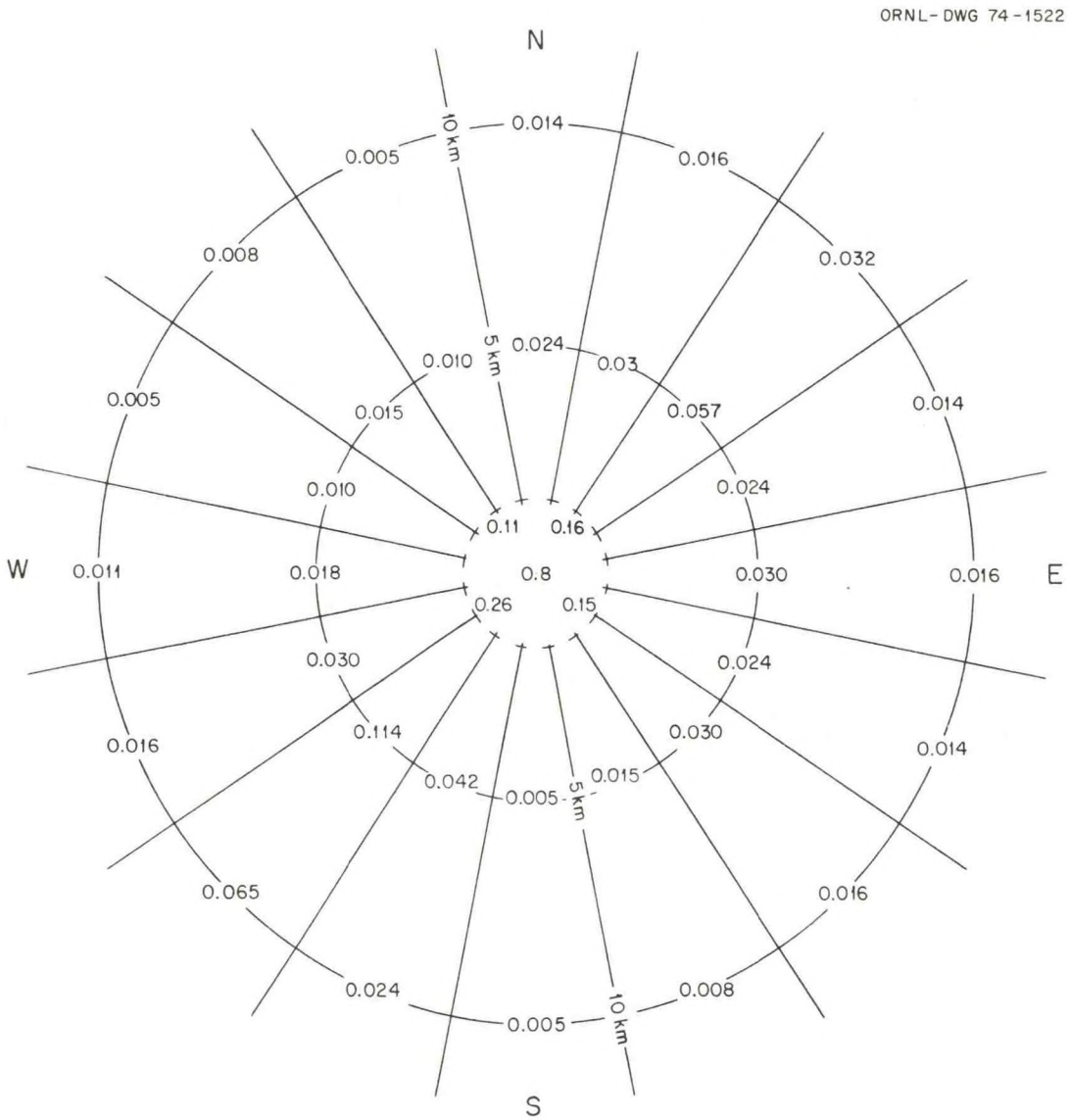

Figure 3: Average annual ground level water concentration (g/m^3) due to cooling towers at ORGDP.

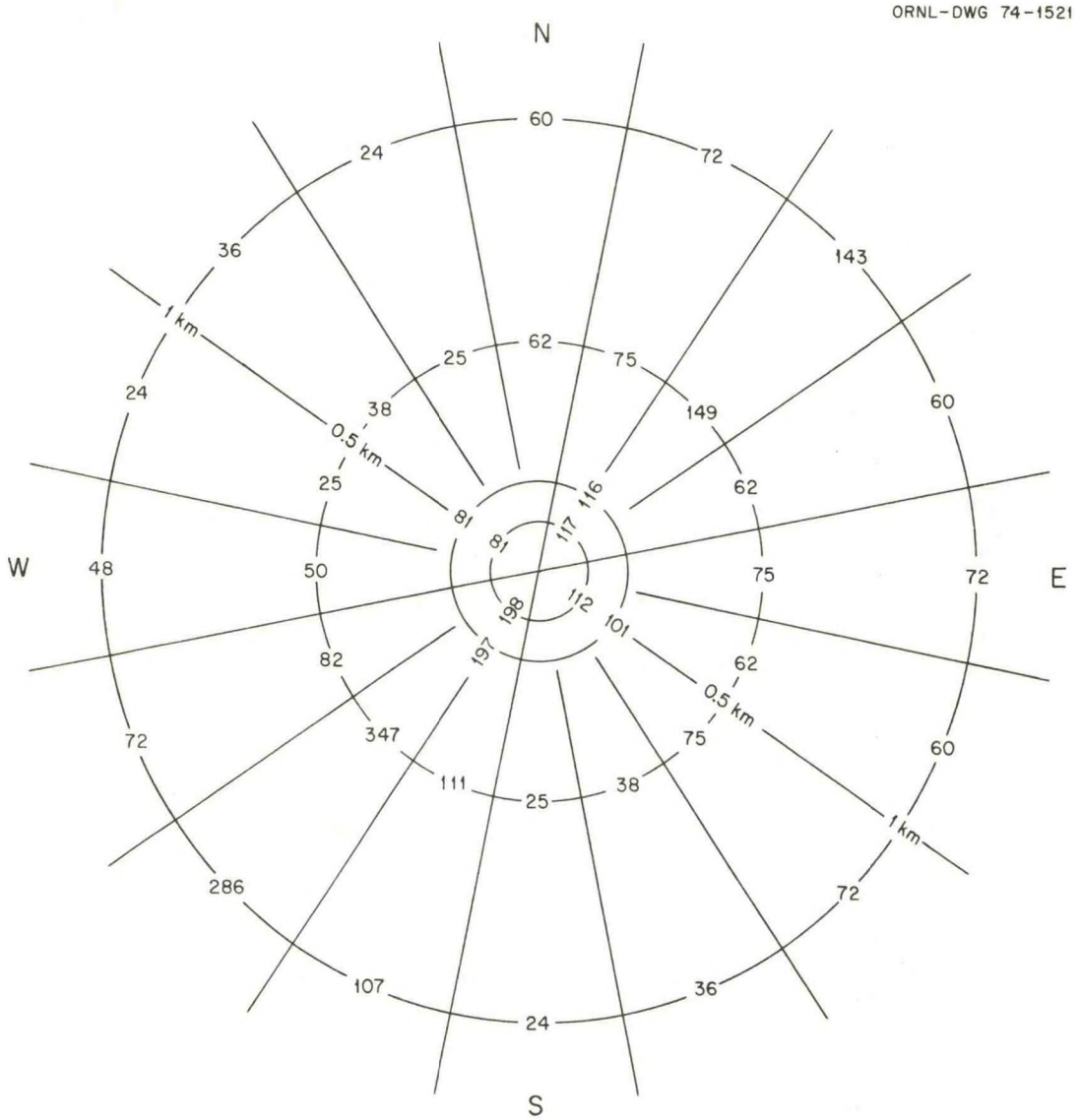

Figure 4a: Extra hours per year of fog caused by cooling tower operation, excluding cases when rain or fog naturally occurs.

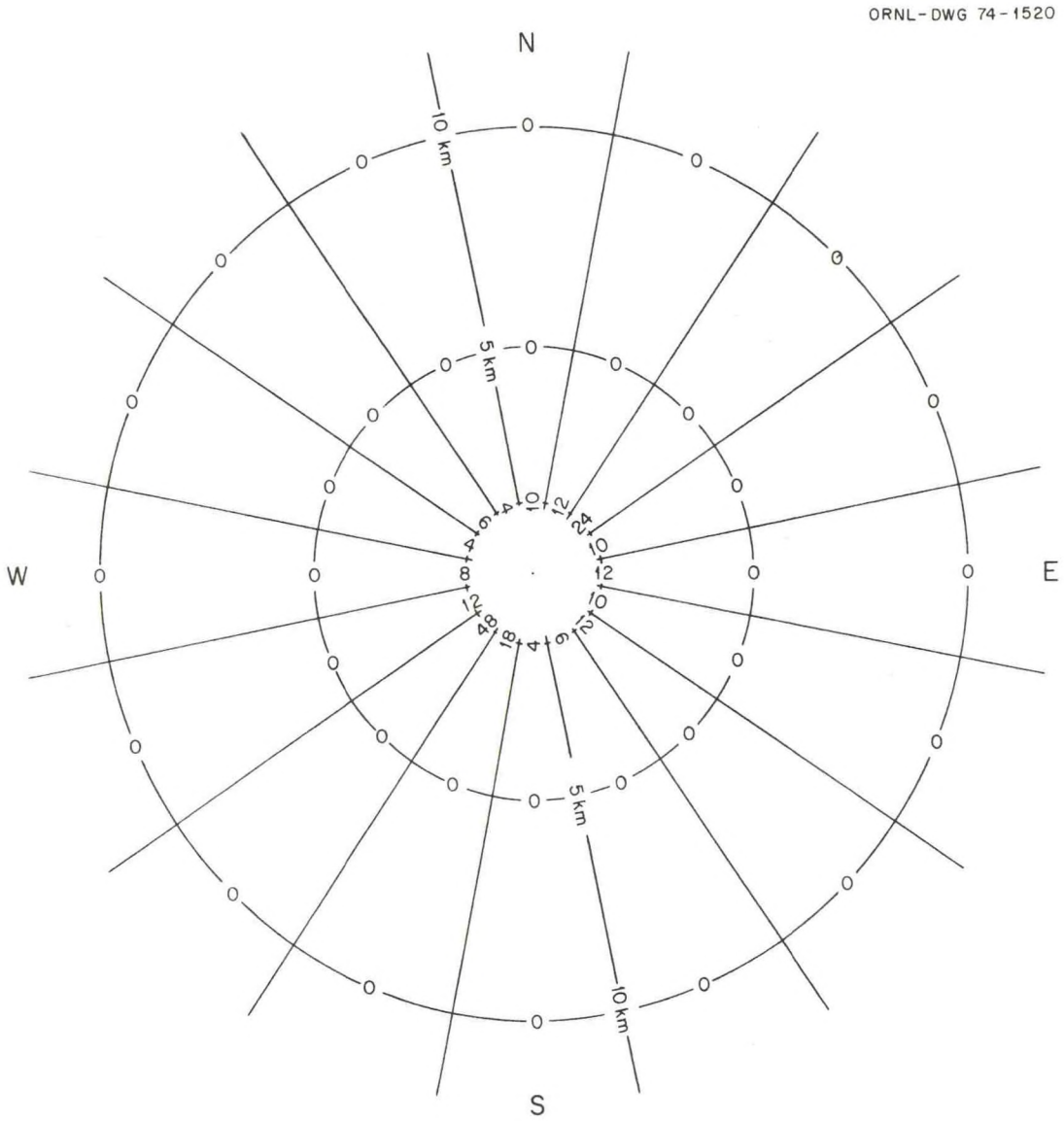

Figure 4b: Same as Figure 4a, but with expanded scale.

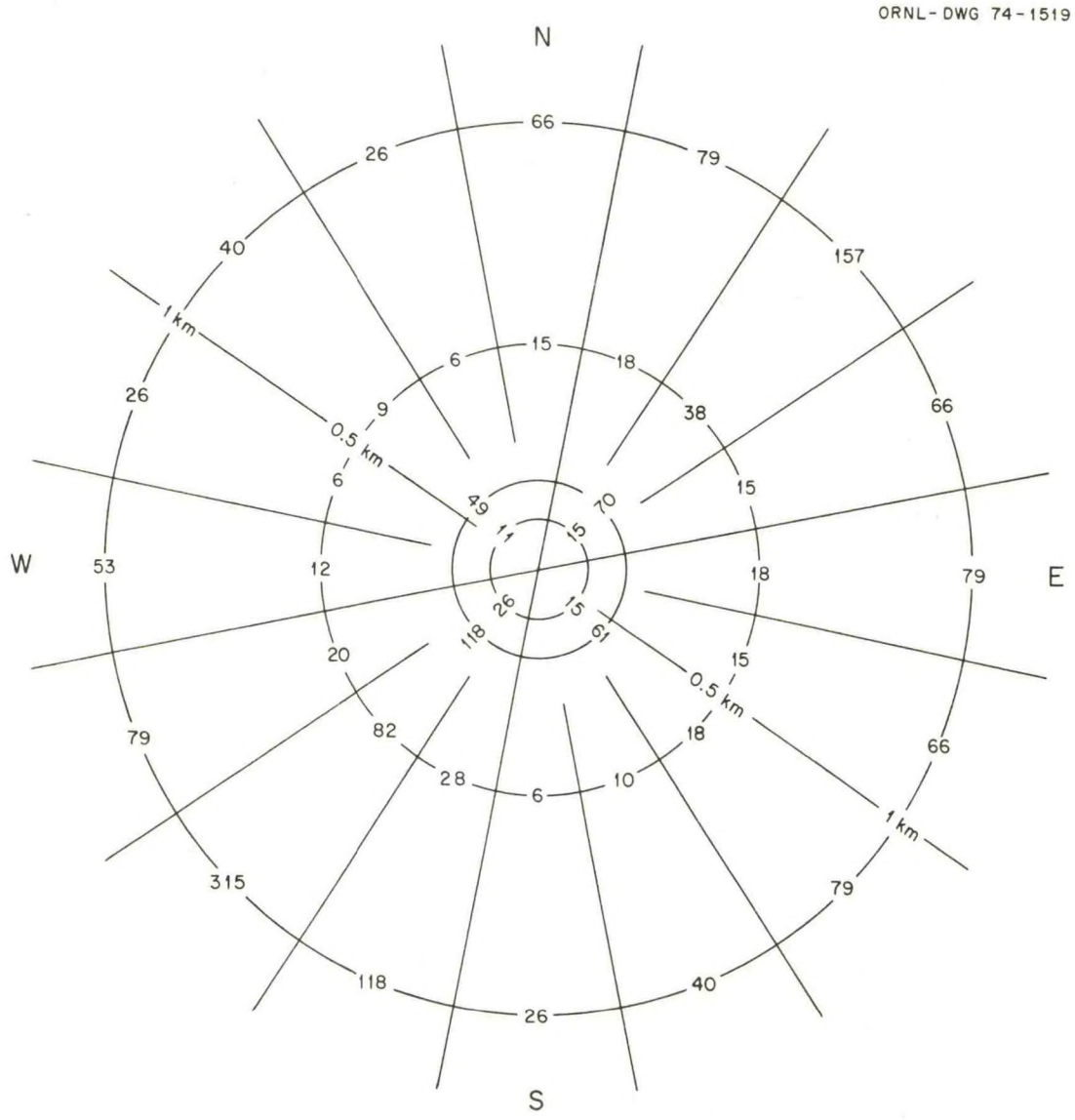

Figure 5a: Hours per year that the cooling tower fog augments naturally-occurring rain or fog.

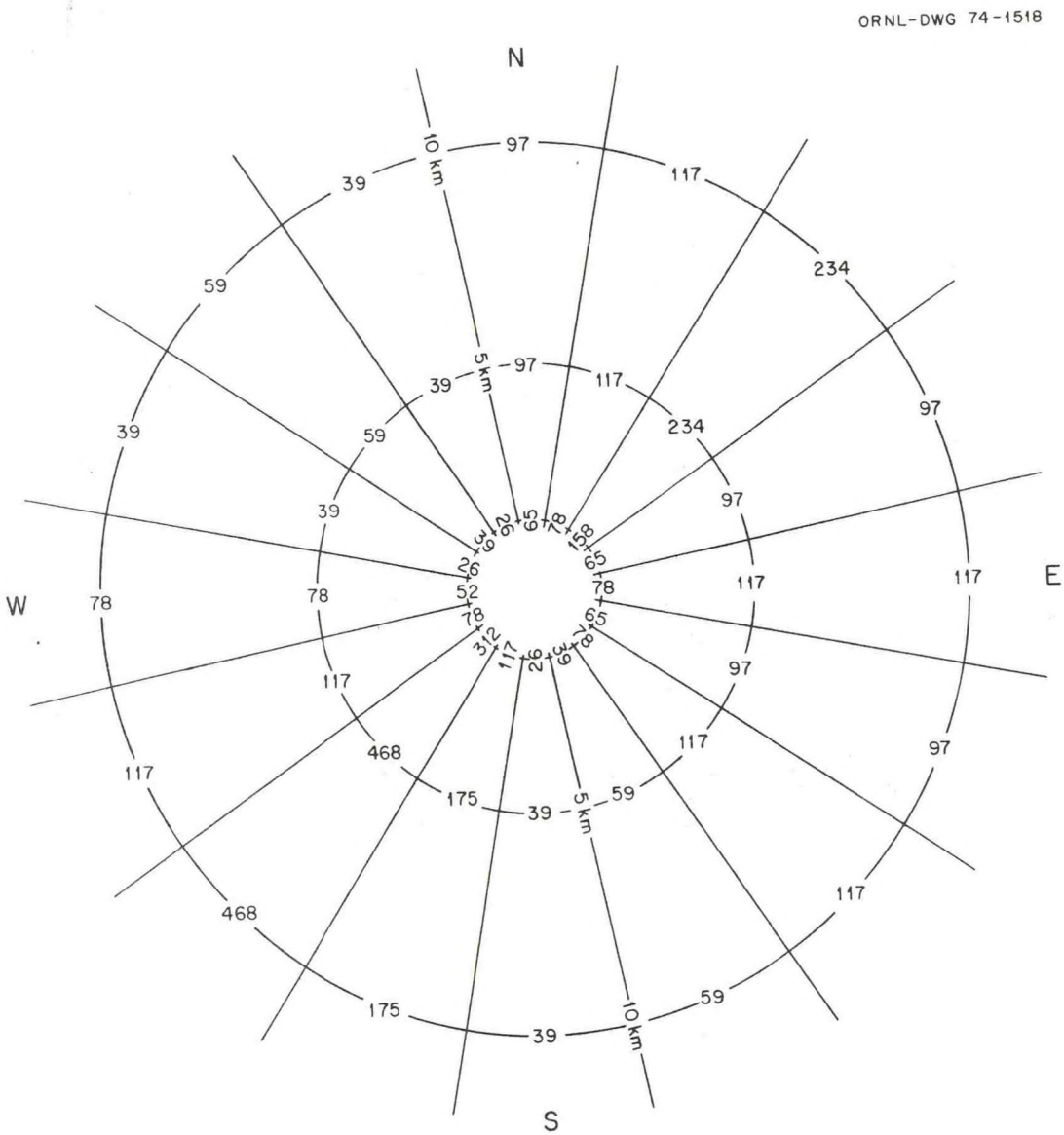

Figure 5b: Same as Figure 5a, but with expanded scale.

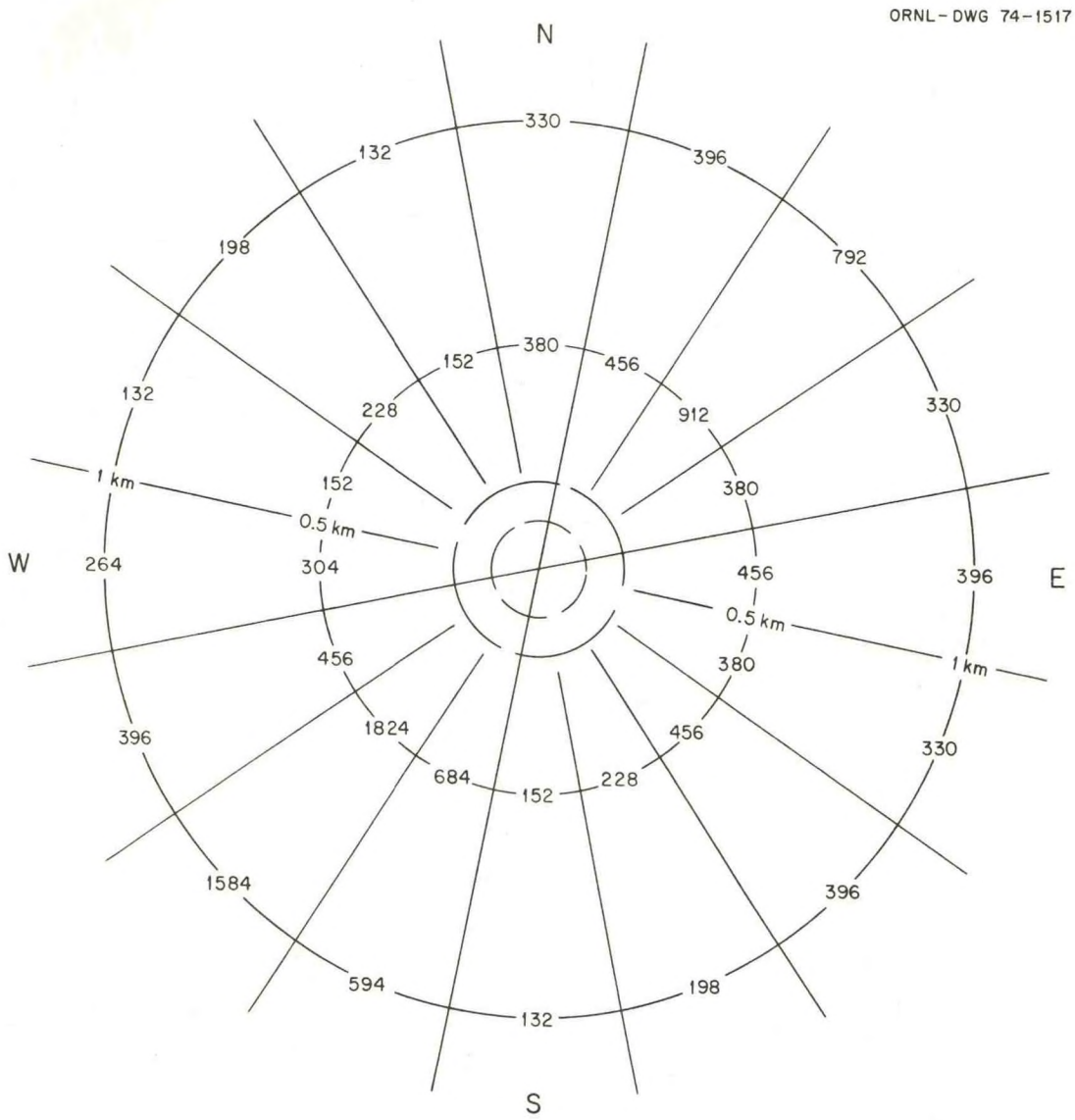

Figure 6a: Hours per year that a visible plume can be seen aloft.

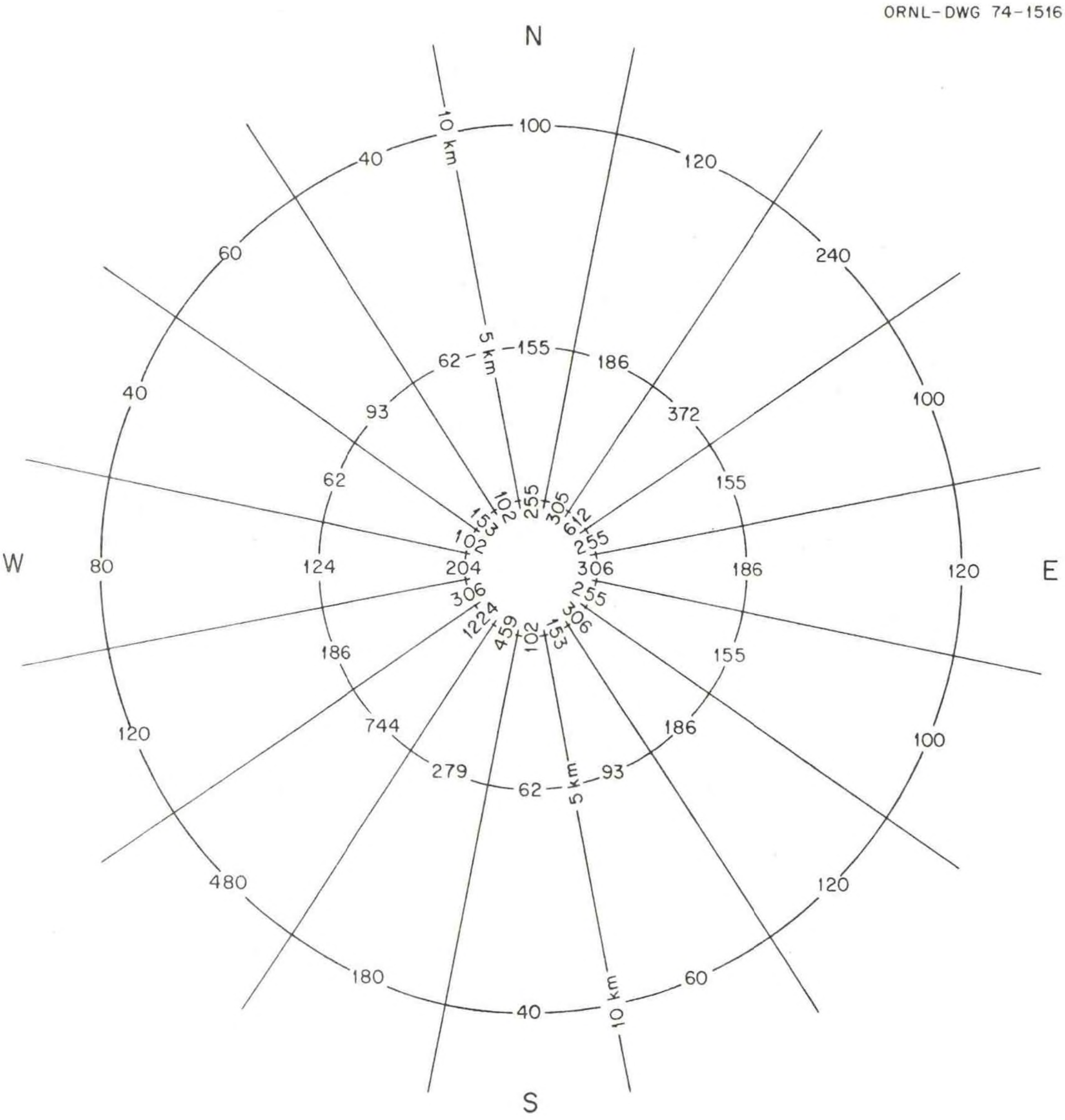

Figure 6b: Same as Figure 6a, but with expanded scale.

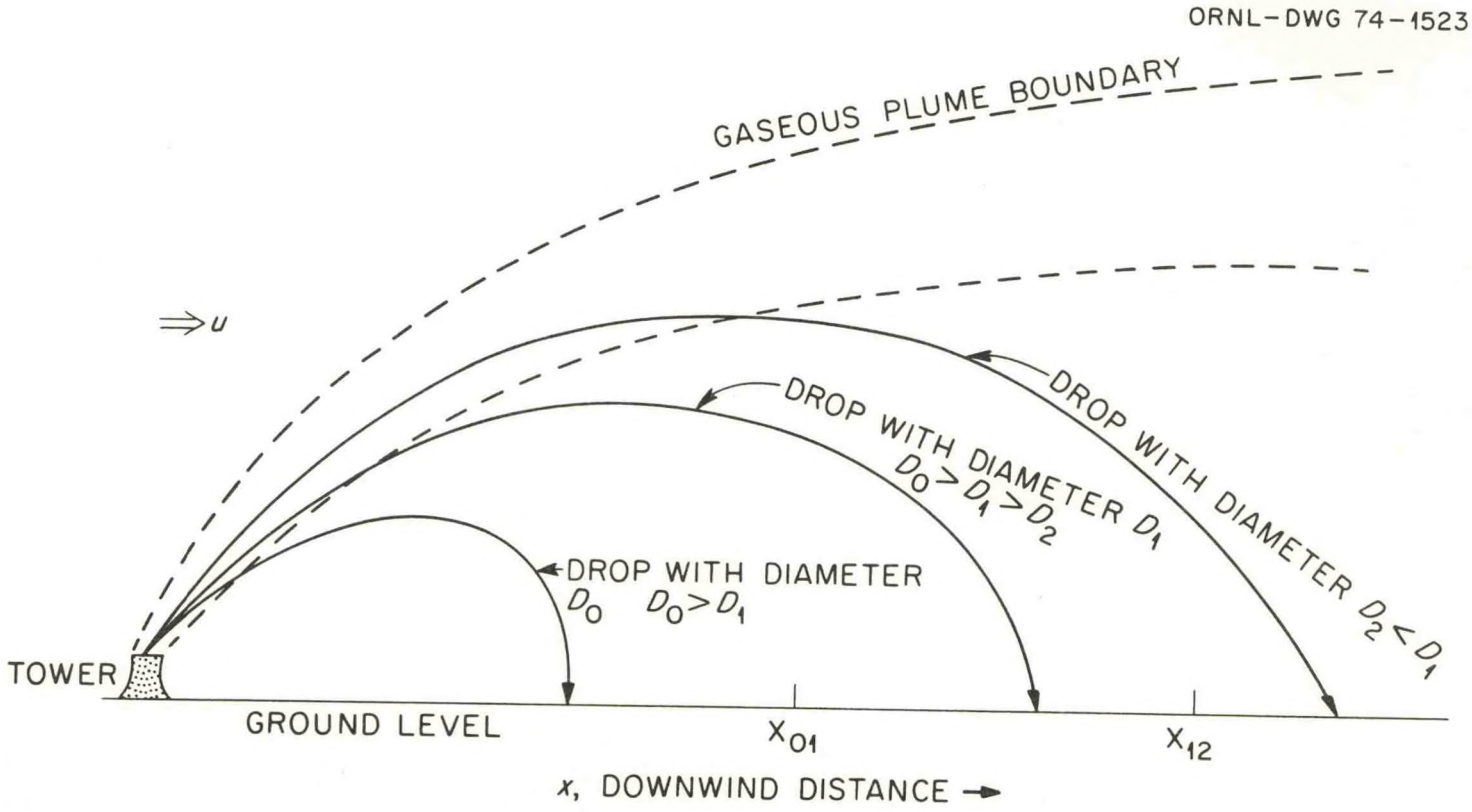

Figure 7: Schematic drawing of drift drop trajectories. Drops with diameter D_1 are assumed to be deposited uniformly between distances x_{01} and x_{12}.

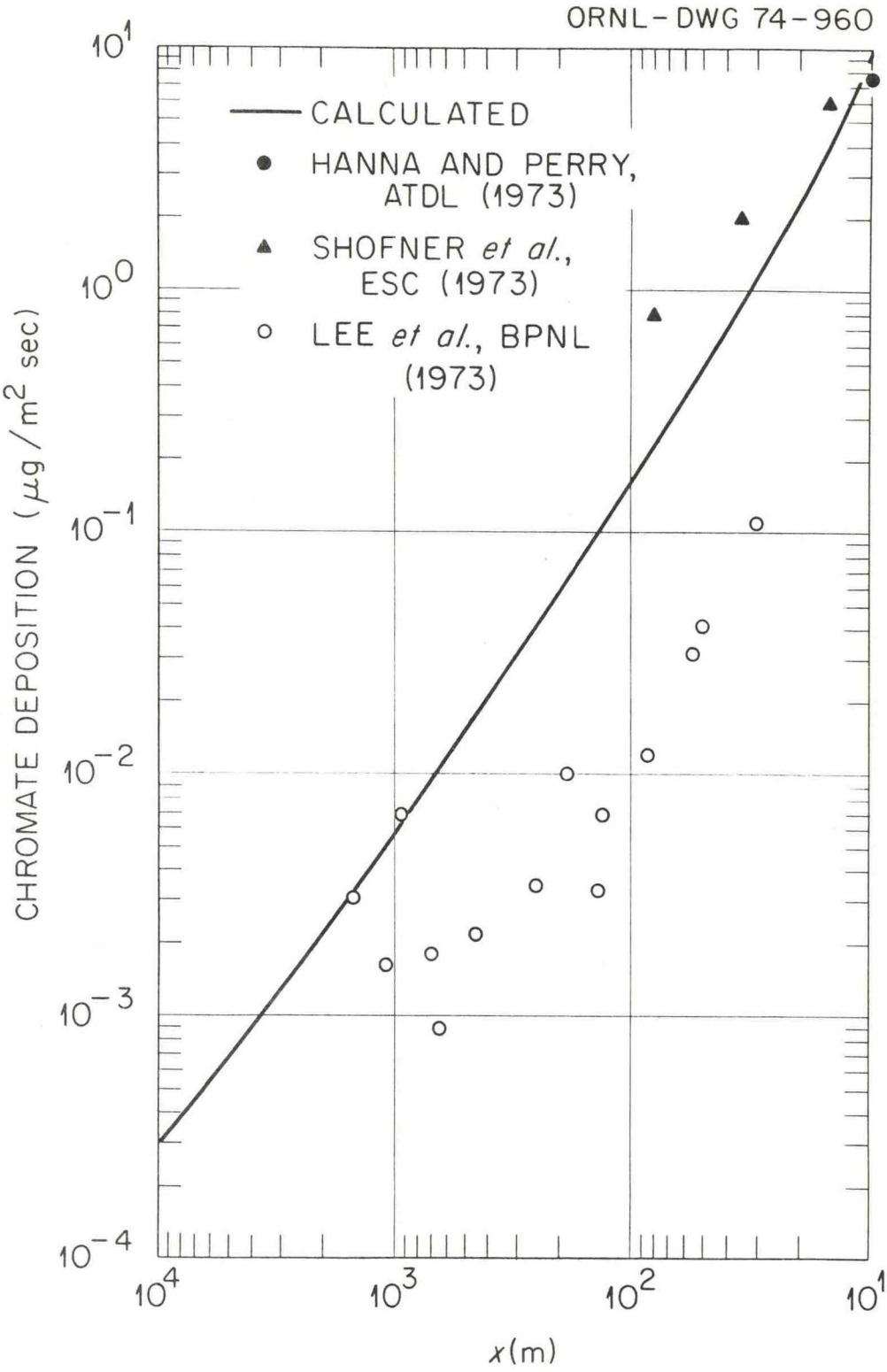

Figure 8: Chromate deposition rate, observed and calculated, during the June 1973 experiment.

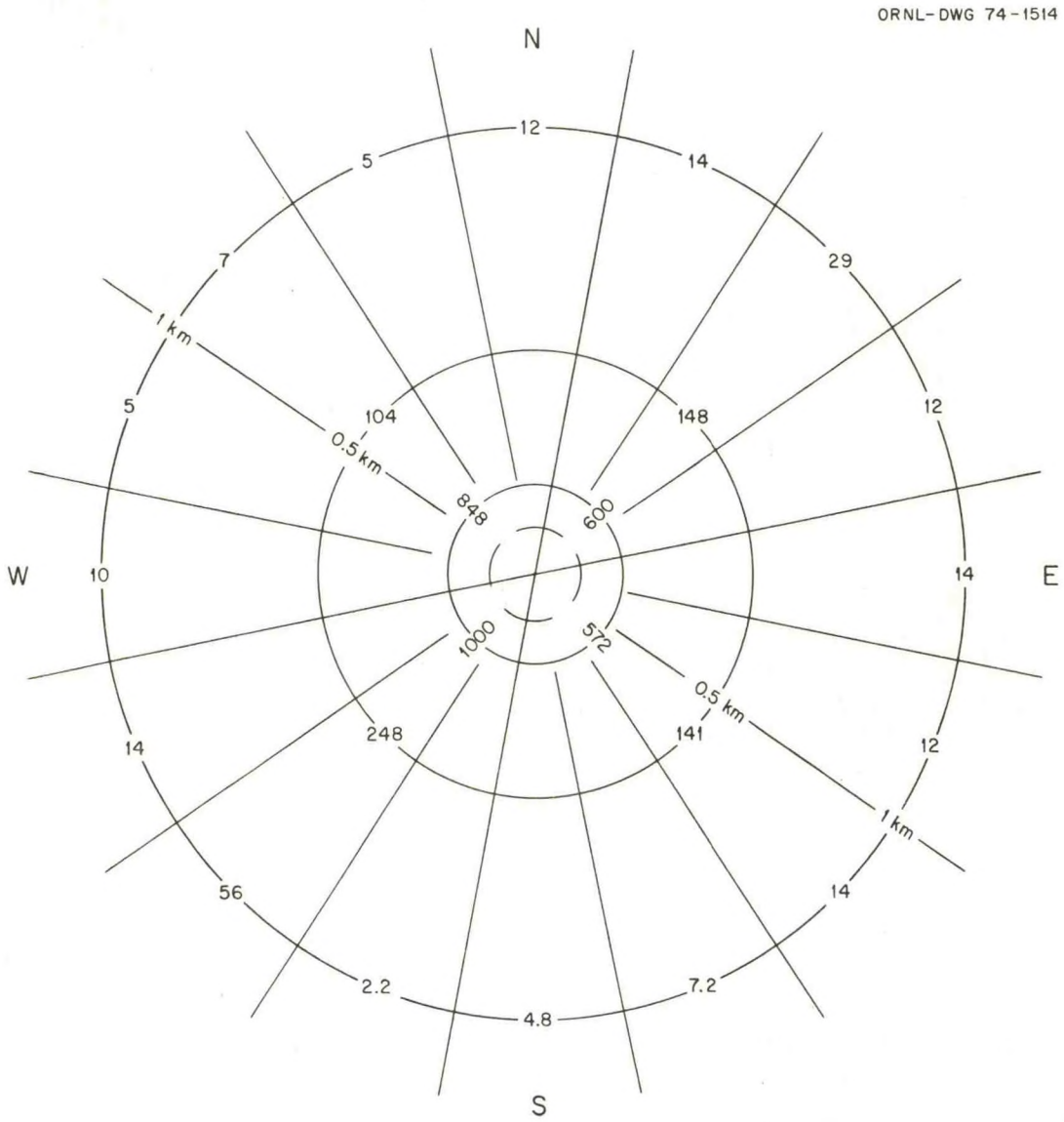

Figure 9a: Annual average deposition rate of chromate, in 10^{-10} g/m^2 sec.

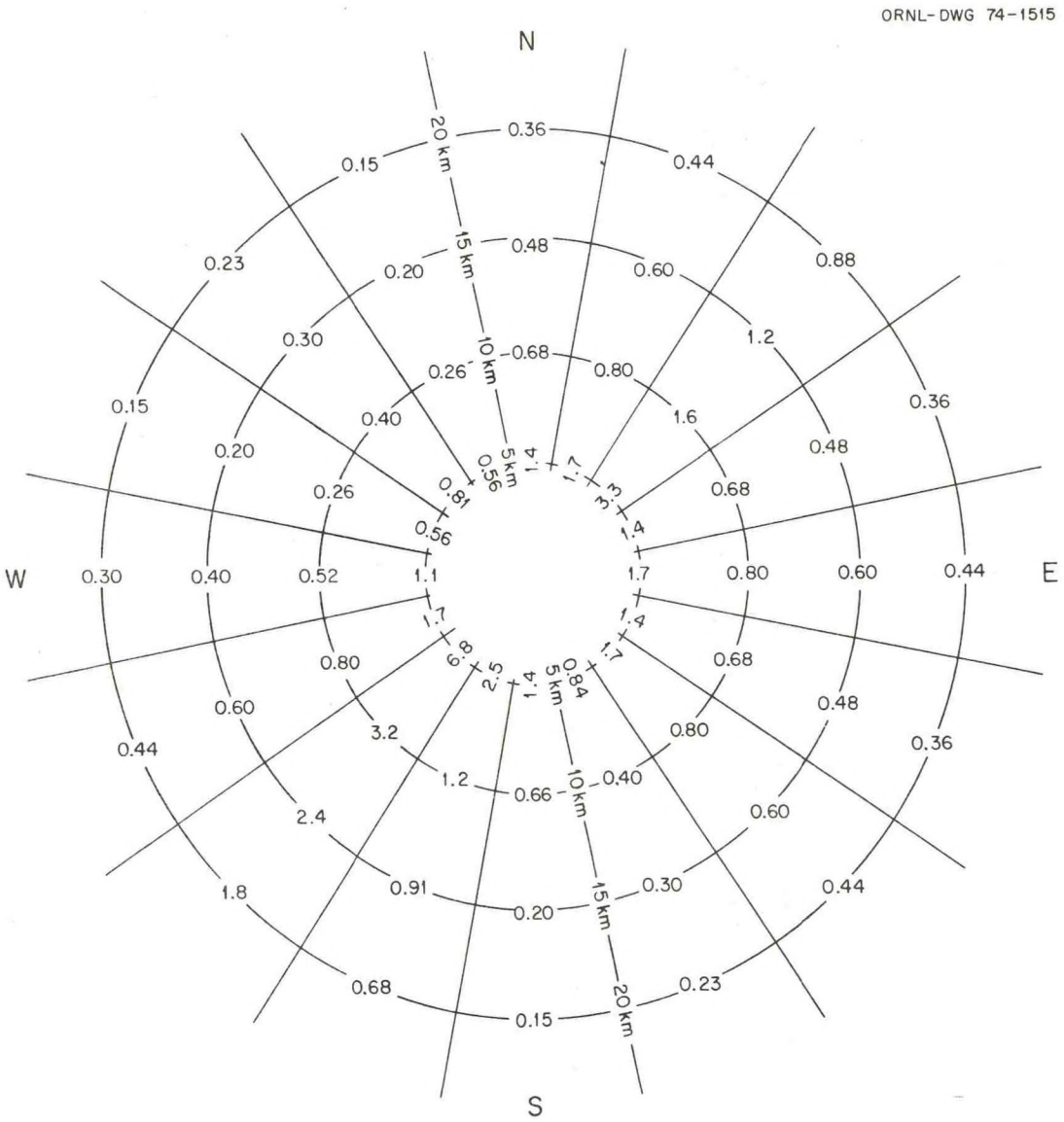

Figure 9b: Annual average deposition rate of chromate, in 10^{-10} g/m^{2}sec.